THE JOURNAL OF BIOLOGICAL CHEMISTRY VOL. 290, NO. 14, pp. 8925–8937, April 3, 2015
© 2015 by The American Society for Biochemistry and Molecular Biology, Inc. Published in the U.S.A.

Formation of Disulfide Bridges Drives Oligomerization, Membrane Pore Formation, and Translocation of Fibroblast Growth Factor 2 to Cell Surfaces*

Received for publication, October 29, 2014, and in revised form, February 17, 2015 Published, JBC Papers in Press, February 18, 2015, DOI 10.1074/jbc.M114.622456

Hans-Michael Müller[‡], Julia P. Steringer[‡], Sabine Wegehingel[‡], Stephanie Bleicken[§¶], Maximilian Münster[‡], Eleni Dimou[‡], Sebastian Unger[‡], Georg Weidmann[‡], Helena Andreas[‡], Ana J. García-Sáez[§¶], Klemens Wild[‡], Irmgard Sinning[‡], and Walter Nickel[‡1]

From the [‡]Heidelberg University Biochemistry Center, 69120 Heidelberg, Germany, [§]Interfaculty Institute for Biochemistry, University of Tübingen, 72076 Tübingen, Germany, and [¶]Max Planck Institute for Intelligent Systems, 70569 Stuttgart, Germany

Background: FGF2 translocation across plasma membranes depends on phosphoinositide-dependent oligomerization and membrane pore formation.
Results: Two unique surface cysteines are critical for efficient FGF2 oligomerization, membrane pore formation, and FGF2 secretion from cells.
Conclusion: Formation of intermolecular disulfide bridges drives phosphoinositide-dependent FGF2 oligomerization at plasma membranes.
Significance: A new *cis* element critical for unconventional secretion of FGF2 was identified and validated.

Fibroblast growth factor 2 (FGF2) is a key signaling molecule in tumor-induced angiogenesis. FGF2 is secreted by an unconventional secretory mechanism that involves phosphatidylinositol 4,5-bisphosphate-dependent insertion of FGF2 oligomers into the plasma membrane. This process is regulated by Tec kinase-mediated tyrosine phosphorylation of FGF2. Molecular interactions driving FGF2 monomers into membrane-inserted FGF2 oligomers are unknown. Here we identify two surface cysteines that are critical for efficient unconventional secretion of FGF2. They represent unique features of FGF2 as they are absent from all signal-peptide-containing members of the FGF protein family. We show that phosphatidylinositol 4,5-bisphosphate-dependent FGF2 oligomerization concomitant with the generation of membrane pores depends on FGF2 surface cysteines as either chemical alkylation or substitution with alanines impairs these processes. We further demonstrate that the FGF2 variant forms lacking the two surface cysteines are not secreted from cells. These findings were corroborated by experiments redirecting a signal-peptide-containing FGF family member from the endoplasmic reticulum/Golgi-dependent secretory pathway into the unconventional secretory pathway of FGF2. *Cis* elements known to be required for unconventional secretion of FGF2, including the two surface cysteines, were transplanted into a variant form of FGF4 without signal peptide. The resulting FGF4/2 hybrid protein was secreted by unconventional means. We propose that the formation of disulfide bridges drives membrane insertion of FGF2 oligomers as intermediates in unconventional secretion of FGF2.

Fibroblast Growth Factor 2 (FGF2) is a signaling molecule with fundamental roles in both tumor-induced angiogenesis (1) and as a survival factor of tumor cells (2). The latter process is based upon the ability of FGF2 to inhibit tumor cell apoptosis by an autocrine secretion-signaling loop. To exert these defined extracellular functions, FGF2 is secreted by an ER[2]/Golgi-independent mechanism (3–6). Various kinds of unconventional secretory pathways from eukaryotic cells have been described (7, 8) with FGF2 being the classical example for the type I pathway of unconventional secretion (7). This secretory mechanism is based upon direct translocation of cargo across the plasma membrane mediated by $PI(4,5)P_2$-dependent membrane insertion of FGF2 oligomers (3, 9, 10). Membrane-inserted forms of FGF2 have been interpreted as intermediates of membrane translocation (3, 10, 11). Directionality of this process is mediated by cell surface membrane-proximal heparan sulfate proteoglycans that are required to complete membrane translocation into the extracellular space resulting in the exposure of FGF2 on cell surfaces (12, 13).

Based on previous work, a lipidic membrane pore was proposed to be induced by $PI(4,5)P_2$-dependent FGF2 oligomerization (10). In this model, the $PI(4,5)P_2$ binding pockets of individual FGF2 subunits were suggested to be in the periphery of such oligomers to allow for interactions with the headgroups of $PI(4,5)P_2$ membrane lipids (7, 11). A role of membrane-inserted oligomers as intermediates in FGF2 secretion (10) is also consistent with the fact that only folded forms of FGF2 qualify for membrane translocation (14, 15). Furthermore, Tec kinase-mediated tyrosine phosphorylation of FGF2 was shown to stimulate both membrane insertion of FGF2 oligomers (10) and efficient secretion of FGF2 from cells (16). Because both recruitment and activation of Tec kinase at the inner leaflet of

* This work was supported by the German Research Council (DFG-SFB 638, DFG-SFB/TRR 83, and DFG-GRK1188), the AID-NET program of the Federal Ministry for Education and Research of Germany, and the Deutsche Forschungsgemeinschaft cluster of excellence CellNetworks.
[1] To whom correspondence should be addressed: Heidelberg University Biochemistry Center (BZH), Im Neuenheimer Feld 328, 69120 Heidelberg, Germany. Tel.: 49-6221-545425; Fax: 49-6221-544366; E-mail: walter.nickel@bzh.uni-heidelberg.de.

[2] The abbreviations used are: ER, endoplasmic reticulum; GUV, giant unilamellar vesicles; NEM, *N*-ethylmaleimide; pCMF, *para*-carboxymethylphenylalanine; $PI(4,5)P_2$, phosphatidylinositol 4,5-bisphosphate.

This is an Open Access article under the CC BY license.

the plasma membrane are regulated by the phosphoinositide PI(3,4,5)P_3 (17), the role of Tec kinase in FGF2 secretion may in part explain the observation that phosphatidylinositol 3-kinases, the enzymes that synthesize phosphatidylinositol-3,4,5-trisphosphate, are up-regulated in many cancers (18).

The current study provides the first insights into molecular determinants that govern the formation of membrane-inserted FGF2 oligomers as membrane translocation intermediates in unconventional secretion. Based on a systematic sequence comparison of all members of the FGF family, we identified two surface cysteines in FGF2 that are absent from all FGF family members with signal peptides for ER/Golgi-dependent secretion. We provide direct evidence for the formation of intermolecular disulfide bridges during FGF2 oligomerization and demonstrate a direct role for the two surface cysteines in PI(4,5)P_2-dependent membrane pore formation. Consistently, substitution of surface cysteines by alanines inhibits unconventional secretion of FGF2 from cells. With the results from the current study, three *cis* elements have been identified in FGF2 that are required for unconventional secretion. These are the basic residues that form the binding pocket for PI(4,5)P_2 (4, 9, 19), the tyrosine residue that is targeted by Tec kinase (3, 7, 16), and the two surface cysteines involved in disulfide formation (this study). The critical relevance of these *cis* elements in FGF2 secretion was further corroborated by experiments testing whether they are transplantable. This was achieved by generating a variant form of FGF4, a FGF family member with a signal peptide that is secreted along the ER/Golgi-dependent route. After transplantation of all three *cis* elements from FGF2 into the appropriate positions in FGF4 and removal of the FGF4 signal peptide, a FGF4/2 hybrid protein was generated that was found secreted by unconventional means. These findings establish the three *cis* elements in FGF2 including the two surface cysteines described in the current study to represent critical molecular determinants of unconventional secretion.

EXPERIMENTAL PROCEDURES

Expression and Purification of Recombinant Proteins—The recombinant proteins FGF2-Y81pCMF and FGF2-Y81pCMF-C77A/C95A were expressed in *Escherichia coli* W3110Z1 cells using the expression vector pQE30 (Qiagen). To generate FGF2 variant forms in which tyrosine 81 was substituted with *p*-carboxylmethylphenylalanine (pCMF), codon 82 (encoding tyrosine 81) was replaced by an amber stop codon followed by transformation of W3110Z1 cells carrying the plasmid pEVOL-pCMF (20). Protein expression was performed in 2×YT medium containing 1 mM pCMF (custom synthesis by ENAMINE Ltd.) for 16 h at 25 °C as described (20). All proteins were His-tagged at the N terminus and affinity-purified using standard procedures (10). For scanning fluorescence cross-correlation experiments (see below), FGF2 constructs (FGF2-Y81pCMF and FGF2-Y81pCMF-C77A/C95A) were generated carrying a C-terminal *Staphylococcus aureus* SortaseA recognition site (LPSTG-*XX*; *X* stands for any amino acid). Using a pQE30 expression vector (Qiagen), the corresponding His-tagged proteins were expressed and purified according to standard procedures (10).

Fluorescent Labeling of FGF2 Variants Forms Using Sortagging—To label recombinant variant forms of FGF2 we used C-terminal sortagging (21). *S. aureus* Δ59 SortaseA was expressed and purified using an N-terminal His_6 tag as described above. His_6-FGF2-LPSTG-XX variants (FGF2-Y81pCMF and FGF2-Y81pCMF-C77A/C95A; 10 μM each) were enzymatically modified in Sortase buffer (50 mM Tris, pH 7.5, 150 mM NaCl, 10 mM $CaCl_2$, 10% (w/v) glycerol) using 10 μM *S. aureus* Δ59 SortaseA and a 10-fold excess of either G_5C-Atto488 or G_5C-Atto655 (100 μM). Samples were incubated for 14 h at 37 °C. After centrifugation (20.000 × *g*; 10 min; 25 °C), removal of excess G_5C-Atto488/G_5C-Atto650 peptides was performed using Econo-Pac 10DG desalting columns (Bio-Rad).

Preparation of Liposomes—All lipids were purchased from Avanti Polar Lipids and stored under argon. Phosphatidylcholine, phosphatidylinositol, and phosphatidylethanolamine were from bovine liver, phosphatidylserine and PI(4,5)P_2 were derived from porcine brain, cholesterol was from ovine wool, and sphingomyelin was from poultry eggs. Lissamine rhodamine B-labeled phosphatidylethanolamine (16:0) was a synthetic product. Chloroform-dissolved lipid mixtures were first dried under a gentle nitrogen stream and further dried under a vacuum for 1.5 h to yield a homogeneous lipid film. Lipids were resuspended in buffer (150 mM KCl, 25 mM HEPES, pH 7.4, 10% (w/v) sucrose) at 45 °C to form liposomes with a final lipid concentration of 4 mM (biochemical interaction experiments) or 8 mM (fluorescence dequenching experiments). Liposomes were subjected to 10 freeze/thaw cycles and 21 size extrusion steps (400-nm pore size; Avanti Polar Lipids mini-extruder). Liposome preparations were analyzed by dynamic light scattering, indicating a range of 200–400 nm in diameter.

Scanning Fluorescence Cross-correlation Spectroscopy to Study Oligomerization of FGF2 on PI(4,5)P_2-containing Giant Unilamellar Vesicles—Giant unilamellar vesicles (GUVs) with a plasma-membrane-like lipid composition containing 2 mol % of PI(4,5)P_2 were formed at 45 °C in sucrose (305 mosmol/kg) using electro-swelling on platinum electrodes (10 Hz, 1.5 V for 40 min, 2 Hz, 1.5 V for 20 min (10)). Three variants of sortagged FGF2 were used, FGF2-Y81pCMF with wild-type surface cysteines, FGF2-Y81pCMF with alkylated surface cysteines, and FGF2-Y81pCMF-C77A/C95A. In each case, two versions of sortagged proteins were generated carrying either LPSTG-Atto488 or LPSTG-Atto655 at the C terminus (see above). For alkylation, His_6-FGF2-Y81pCMF-LPSTG-Atto488 and His_6-FGF2-Y81pCMF-LPSTG-Atto655 (420 nM each) were preincubated with 1.68 μM NEM (giving a 2-fold molar excess of NEM over FGF2 surface cysteines) in 25 mM HEPES, pH 7.4, 150 mM NaCl at 25 °C for 30 min. LPSTG-Atto488- and LPSTG-Atto655-tagged versions of each FGF2 variant form were incubated with GUVs at a final concentration of 36 nM. After 60 min of incubation at 22 °C, two-focus scanning FCCS measurements were conducted at 22 °C on a LSM710 confocal fluorescence microscope using a C-Apochromat 40 × 1.2 water immersion objective (Zeiss, Jena, Germany). Argon ion (488 nm) and HeNe (633 nm) lasers were used for sample excitation. Photon detection was done with avalanche photodiodes of the ConFocor 3 module, and photon arrival times were recorded in

the photon mode of the hardware correlator Flex 02-01D/C. Measurements and data analysis were done as described previously (10, 22). Because labeling efficiencies obtained by sortagging (see above) were relatively low, scanning fluorescence cross-correlation data are shown as % cross-correlation and as diffusion constants (Fig. 2). Note that cross-correlation data comparing different protein preparations with distinct labeling efficiencies are not directly comparable. By contrast, the determination of diffusion constants is independent of labeling efficiencies.

Analysis of Membrane-bound FGF2 Oligomers Employing Native Acidic PAGE and SDS-PAGE—FGF2 (20 μM) and liposomes (4 mM total lipid) with a plasma membrane-like lipid composition containing 2 mol % of PI(4,5)P_2 (9, 23) were incubated at 25 °C in a final volume of 100 μl of buffer (150 mM KCl, 25 mM HEPES, pH 7.4). After the incubation times indicated, *N*-ethyl maleimide (100 μM final concentration) was used to alkylate free remaining thiols of cysteine residues. Sedimented liposomes washed with 100 μl of buffer (150 mM KCl, 25 mM HEPES, pH 7.4) were dissolved in 24 μl of the detergent C12E8 (octaethylenglycol-monododecyl ether; 5%). Samples were incubated for 30 min at 37 °C (including 40 mM DTT where indicated). A native acidic gel electrophoresis method developed to separate basic proteins (24) was adapted to the Bio-Rad Mini-PROTEAN electrophoresis system. 12 μl of the sample were mixed with 4 μl of sample buffer and loaded onto acidic gels (3% stacking, 12% separation gel; acrylamide-bisacrylamide ratio 29:1). Of the remaining 12-μl sample, 6 μl were mixed with 6 μl of SDS sample buffer with β-mercaptoethanol (350 mM; reducing) or without β-mercaptoethanol (non-reducing), heated for 5 min at 95 °C, and analyzed on 4–20% gradient SDS-PAGE. In addition to samples incubated in the presence of PI(4,5)P_2-containing membranes, control samples incubated in the absence of membranes were otherwise treated identically, and 40% of each sample were analyzed as well. All gels were stained with Coomassie (InstantBlue, Expedeon).

Analysis of Membrane Pore Formation—Membrane pore formation by different variant forms of FGF2 was analyzed as described previously (10). Briefly, liposomes with a plasma membrane-like lipid composition containing 2 mol % of PI(4,5)P_2 were prepared in a buffer (100 mM KCl, 25 mM HEPES, pH 7.4, 10% (w/v) sucrose) and supplemented with 100 μM concentrations of the membrane-impermeant fluorophore 5(6)-carboxyfluorescein (Sigma). To remove extraluminal 5(6)-carboxyfluorescein, liposomes were diluted in buffer (150 mM KCl, 25 mM HEPES, pH 7.4) and collected by centrifugation at 15,000 × *g* for 10 min at 20 °C followed by size exclusion chromatography using a PD10 column (GE Healthcare). Importantly, this column was operated in buffer (150 mM KCl, 25 mM HEPES, pH 7.4, 10% (w/v) sucrose, 2% (w/v) glucose) that was titrated with glucose to reach iso-osmolality (840 mosmol/kg). After incubation with various forms of FGF2 (2 μM) as indicated, fluorescence dequenching was measured using a SpectraMax M5 fluorescence plate reader (Molecular Devices). At the end of each experiment, Triton X-100 (0.2% (w/v) final concentration) was added to measure maximal dequenching used to normalize data.

Quantification of FGF2 Secretion from Cells Using Cell Surface Biotinylation—Stable CHO cell lines expressing either FGF2-GFP, FGF2-GFP-C77A/C95A, a PI(4,5)P_2 binding mutant of FGF2-GFP (FGF2-GFP-K127Q/R128Q/K133Q), or GFP were cultivated in the presence of doxycycline (to induce protein expression) for 16 h at 37 °C (resulting in a confluency of ~70%). After removal of the growth medium, cells were washed twice with PBS and incubated with 0.75 mg/ml membrane-impermeable biotinylation reagent (EZ-Link Sulfo-NHS-SS-Biotin, Pierce; dissolved in 10 mM triethanolamine, pH 9.0, 150 mM NaCl, 2 mM $CaCl_2$) for 30 min at 4 °C. After quenching of excess biotin with 100 mM glycine (dissolved in PBS) and 2 PBS washing steps, cells were lysed with 1% Nonidet P-40 (in 50 mM Tris/HCl, pH 7.7, 62.5 mM EDTA, 0.4% deoxycholate, protease inhibitor mixture (Roche Applied Science)), and insoluble material was removed by centrifugation (10 min, 20,000 × *g*, 4 °C). Biotinylated and non-biotinylated fractions were separated on streptavidin beads (UltraLink immobilized streptavidin; Pierce). Bound material was eluted with SDS sample buffer and analyzed by Western blotting using affinity-purified anti-GFP antibodies (25) and monoclonal anti-GAPDH antibodies (Lifetech-Ambion). Antigen signals were quantified using an infrared imaging system (LI-COR Biosciences).

Secretion Analysis of Various FGF Fusion Proteins Using Cell Surface Biotinylation Assays and Heparin Affinity Purification from Cellular Supernatants—To test whether *cis* elements identified to be required for FGF2 secretion are transplantable into a secretory protein traveling along the ER/Golgi-dependent pathway, we chose FGF4 as a model protein as it shares overall structural similarity with FGF2 (Fig. 1). In addition to FGF2-GFP, we generated constructs encoding a signal-peptide-containing FGF4-GFP fusion protein (SP-FGF4-GFP), a corresponding fusion protein without signal peptide (FGF4-GFP), and various kinds of FGF4/2 hybrid proteins without signal peptide but containing *cis* elements derived from FGF2. Those included two surface cysteines transplanted from FGF2 into the corresponding positions in FGF4 (A132C and F150C) and the FGF2 tyrosine residue targeted by Tec kinase (F136Y) as well as three residues from the FGF2 binding pocket required for binding to PI(4,5)P_2 (S182K, K183R, and N184T). These positions refer to full-length human FGF4 including signal peptide and, therefore, differ from the positions of the alignments shown in Figs. 1*D* where the signal peptide was omitted. Stable CHO cell lines expressing these fusion proteins in a doxycycline-dependent manner were generated by retroviral transduction (25). The subcellular localization of all fusion proteins was characterized by confocal microscopy (Fig. 7). Briefly, protein expression was induced with doxycycline for 24 h. Cells were fixed with paraformaldehyde and stained with wheat germ agglutinin (5 μg/ml, Alexa Fluor 594 conjugate; Life Technologies). Alternatively, cells were first permeabilized for 5 min with 0.1% Triton X-100 followed by incubation with anti-GM130 antibodies used as a Golgi marker (BD Biosciences; catalogue #610822) along with secondary antibodies labeled with Alexa Fluor 546 (Life Technologies). All samples were further stained with Hoechst 33342 (1 μg/ml) to label nuclei. Three-color images were recorded using a Nikon A1R confocal microscope (Fig. 7). Cell surface biotinylation was conducted as described above. In

addition, cellular supernatants were probed for the FGF-GFP fusion proteins indicated because, as opposed to FGF2 (13), FGF4 was known to be secreted into cellular supernatants (5). After clearance at 200 × *g* for 10 min at 4 °C, supernatants were incubated with heparin-Sepharose beads (GE Healthcare #17-0998-01) for 2 h at 4 °C. After extensive washing with PBS, bound protein was eluted with SDS sample buffer and analyzed by SDS-PAGE and quantitative Western blotting using the LI-COR imaging platform. For the analyses shown in Fig. 8, 10% of total cells (input) and 33% for both cell surfaces and cellular supernatants were analyzed per experimental condition.

RESULTS

To identify unique *cis* elements in FGF2, we conducted a systematic multiple sequence alignment based upon ClustalW 2.1 (Fig. 1). This analysis revealed two surface cysteines in FGF2, Cys-77 and Cys-95, that are absent from all other FGF family members with signal peptides for ER/Golgi-dependent secretion (Fig. 1*D*). By contrast, two internal cysteine residues, Cys-33 and Cys-100, were found ubiquitously present across all FGF family members, suggesting that they are of general importance for the conformation and stability of FGF proteins. To test whether the presence of Cys-77 and Cys-95 in FGF2 relates to its ability to reach the extracellular space, we analyzed whether these residues are critical for (i) $PI(4,5)P_2$-dependent oligomerization of FGF2 on membrane surfaces, (ii) membrane insertion of FGF2 oligomers as intermediates in translocation, and (iii) FGF2 secretion from cells.

FGF2 Variant Forms Lacking Functional Surface Cysteines Are Impaired in PI(4,5)P_2-dependent Oligomerization—In a first set of experiments we aimed at analyzing oligomerization of FGF2 on membrane surfaces under native conditions employing scanning fluorescence cross correlation spectroscopy (22, 26) (Fig. 2). A phosphomimetic form of FGF2 was used that mimics the product of Tec kinase-mediated tyrosine phosphorylation of FGF2, FGF2-Y81pCMF (10). Three variant forms of FGF2-Y81pCMF were analyzed characterized by (i) the presence of surface cysteines, (ii) alkylated surface cysteines, or (iii) alanines substituting surface cysteines. All forms of FGF2-Y81pCMF were labeled by C-terminal sortagging (27) using both green and red dyes to generate two populations of each FGF2 variant form for cross-correlation experiments. After incubation with GUVs containing $PI(4,5)P_2$, oligomerization was monitored by quantifying the percentage of cross-correlation under the experimental conditions indicated (Fig. 2*A*). In addition, diffusion constants characterizing the lateral mobility of all three variant forms of FGF2-Y81-pCMF were determined in GUVs (Fig. 2*B*). As compared with the wild-type form of FGF2-Y81pCMF, both FGF2-Y81pCMF with alkylated surface cysteines and FGF2-Y81pCMF-C77A/C95A were impaired in $PI(4,5)P_2$-dependent oligomerization on membrane surfaces (Fig. 2*A*). Consistently, compared with FGF2-Y81pCMF, both FGF2-Y81pCMF treated with NEM and FGF2-Y81pCMF-C77A/C95A were characterized by higher diffusion constants indicating an impaired ability to oligomerize. These findings suggest a direct role for disulfide bridges promoting oligomerization of FGF2 on membrane surfaces.

As an alternative read-out to analyze FGF2 oligomerization in the presence of $PI(4,5)P_2$-containing membranes, we used native gel electrophoresis as well as non-reducing and reducing SDS gel electrophoresis (Fig. 3). FGF2-Y81pCMF was incubated either in the absence of membranes (*panels A*, *C*, *E*, and *G*) or with $PI(4,5)P_2$-containing liposomes (*panels B*, *D*, *F*, and *H*) for the times indicated. After extraction with detergent, samples were divided and analyzed on native gels (*panels A* and *B*), on non-reducing SDS gels (*panels C* and *D*), or on reducing SDS gels (*panels E* and *F*). In addition, FGF2-Y81pCMF was pretreated with 10 mM DTT before incubation in the absence (Fig. 3, *panel G*) or presence of liposomes (Fig. 3*H*). In the presence of $PI(4,5)P_2$-containing liposomes, FGF2-Y81pCMF oligomers were observed to form in a time-dependent manner with dimers and trimers abundantly present after 30 min of incubation (Fig. 3*B*). Tetramers and higher oligomers were observed at later time points starting at 1 h of incubation (Fig. 3*B*). By contrast, in the absence of membranes, the formation of FGF2-Y81pCMF oligomers was undetectable (Fig. 3, *A*, *C*, *E*, and *G*). To test the presence of intermolecular disulfide bridges in FGF2-Y81pCMF oligomers, the same samples shown in Fig. 3*B* were further analyzed on non-reducing (Fig. 3*D*) and reducing (Fig. 3*F*) SDS gels. Moreover, an experimental condition was added where FGF2-Y81pCMF was pretreated with 10 mM DTT before adding $PI(4,5)P_2$-containing liposomes (Fig. 3*H*). Compared with the analysis on native gels (Fig. 3*B*) a very similar pattern of oligomeric forms of FGF2-Y81pCMF was observed on non-reducing SDS gels (Fig. 3*D*). By contrast, the abundance of oligomeric forms was decreased on reducing SDS gels (Fig. 3*F*) and largely disappeared when FGF2-Y81pCMF was pretreated with DTT before adding membranes (Fig. 3*H*).

In a complementary set of experiments, three different variant forms of FGF2, FGF2-Y81pCMF with wild-type cysteines, FGF2-Y81pCMF with alkylated cysteines, and FGF2-Y81pCMF-C77A/C95A, were incubated with $PI(4,5)P_2$-containing membranes for 6 h. After detergent extraction, each variant form was incubated in the presence of the reducing agent DTT or was mock-treated followed by an analysis on native gels (Fig. 4). These experiments revealed that oligomers of FGF2-Y81pCMF higher than dimers largely disappeared under reducing conditions (Fig. 4*A*, *lane 2 versus lane 3*). Furthermore, FGF2-Y81pCMF with alkylated cysteines as well as FGF2-Y81pCMF-C77A/C95A were virtually incapable of forming oligomers higher than dimers under these conditions (Fig. 4*A*, *lanes 5* and *8*). These effects were also visible when analyzing the consumption of FGF2 monomers during oligomerization. For wild-type FGF2-Y81pCMF, a strong loss of monomer was observed (Fig. 4*A*, *lane 2*) that reappeared upon DTT treatment (Fig. 4*A*, *lane 3*). By contrast, monomer consumption could not be observed for FGF2-Y81pCMF with alkylated cysteines (Fig. 4*A*, *lane 5*) or FGF2-Y81pCMF-C77A/C95A (Fig. 4*A*, *lane 8*). In addition to the representative example shown in Fig. 4*A*, we quantified the results from three independent experiments comparing the quantitative changes of monomers, dimers, trimers, and tetramers under mock and reducing conditions (Fig. 4, *B*, *C*, and *D*). For the wild-type form of FGF2-Y81pCMF, this analysis revealed an increase of monomers and a decrease of oligomeric forms upon treatment with

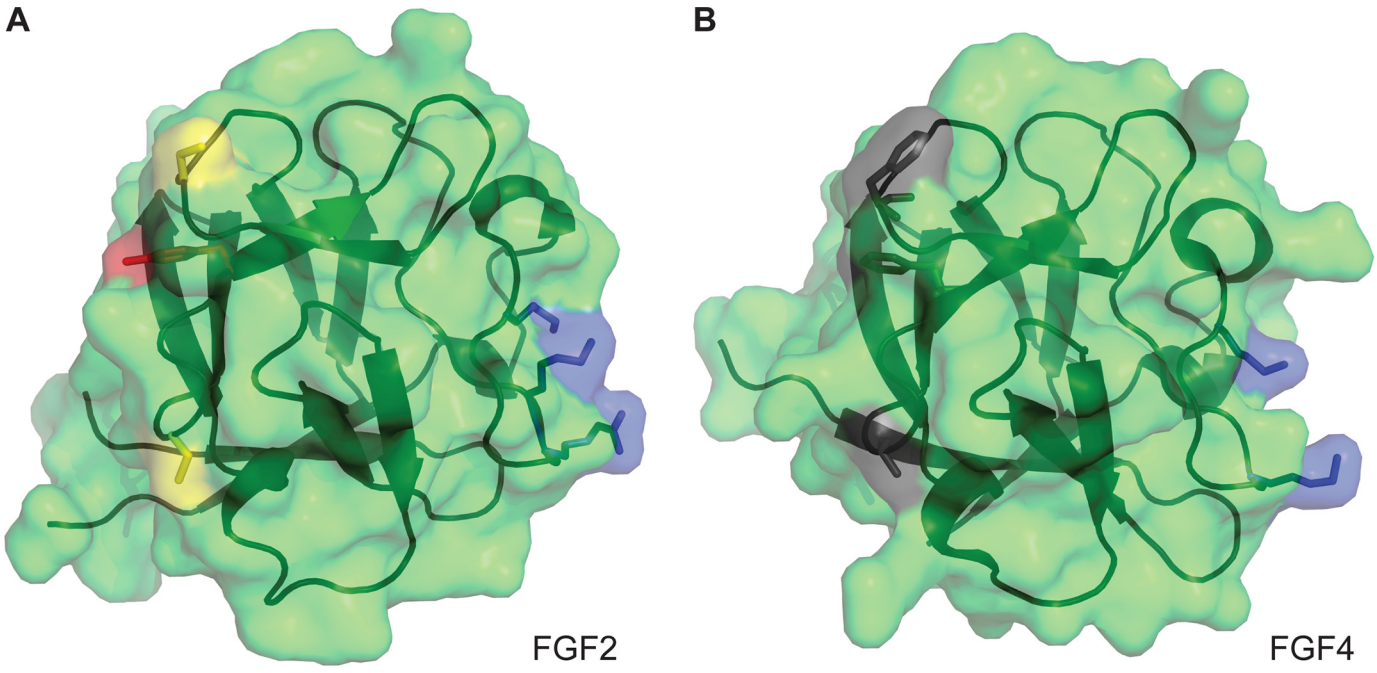

C

```
Conservation
FGF2   AAGSITTLP  AL------PE  DGGSGAFPPG  HFKDPKRLYC  KNG-GFFLRI  HPDGRVDGVR  52
FGF4   VALSLARLP  VAAQPKEAAV  QSGAGDYLLG  -IKRLRRLYC  NVGIGFHLQA  LPDGRIGGAH  58
                                                  33
Conservation
FGF2   KSDPHIKLQ  LQAEERGVVS  IKGVCANRYL  AMKEDGRLLA  SKCVTDECFF  FERLESNNYN  112
FGF4   DTR-DSLLE  LSPVERGVVS  IFGVASRFFV  AMSSKGKLYG  SPFFTDECTF  KEILLPNNYN  117
                              77       81          95       100
Conservation
FGF2   YRSRKYTSW  YVALKRTGQY  KLGSKTGPGQ  KAILFLPMSA  KS                      154
FGF4   YESYKYPGM  FIALSKNGKT  KKGNRVSPTM  KVTHFLPRL-  --                      156
                  127 128     133
```

D

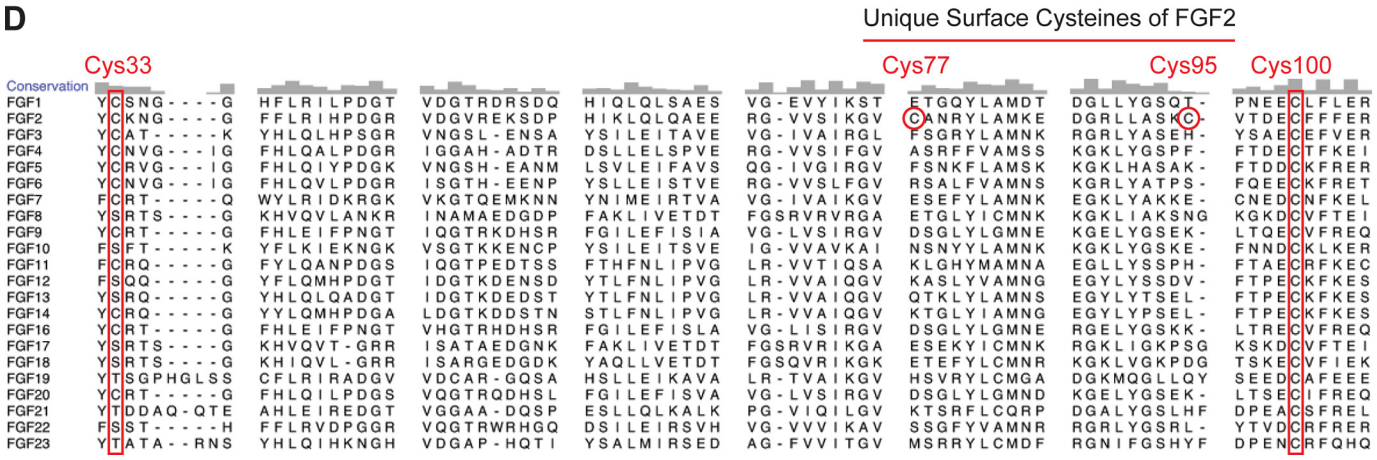

FIGURE 1. **Structural comparison of FGF2 with FGF4, a signal-peptide-containing FGF family member that is secreted through the classical, ER/Golgi-dependent pathway.** In *panels A* and *B*, a combination of space-filling and secondary structure-based models of FGF2 (PDB: 1BFF) and FGF4 (PDB: 1IJT) are shown from a similar perspective emphasizing the overall structural similarity between FGF2 and FGF4. In *panel A*, two surface cysteines in positions 77 and 95 of FGF2 are highlighted in *yellow* that are absent from FGF4 (*panel B*). The corresponding positions in FGF4 are shown in *gray*. In addition, in *panel A*, important *cis* elements in FGF2 are highlighted in *red* (tyrosine 81) and *blue* (basic residues of the $PI(4,5)P_2$ binding pocket). In FGF4 (*panel B*), a phenylalanine residue is present in position 81 (shown in *gray*). The region in FGF2 forming the $PI(4,5)P_2$ binding pocket is highlighted in *blue* (*panel A*). The corresponding region in FGF4 also contains basic residues that are shown in *blue* as well (*panel B*). In *panel C*, a sequence alignment between FGF2 and FGF4 is shown with the two surface cysteines in positions 77 and 95, tyrosine 81 and the $PI(4,5)P_2$ binding pocket of FGF2 being highlighted in the colors used in *panels A* and *B*. Note that amino acid numbering was adjusted to the FGF2 sequence starting with the residue A, which represents the first amino acid of FGF2 after removal of the N-terminal methionine. The N-terminal signal peptide of FGF4 has been omitted from the sequence analysis shown in *panel C*. In *panel D*, a multiple sequence alignment (Clustal Omega) spanning residues 32–105 (numbering based on the 18 kDa form of FGF2) of the human FGF family illustrates that the two surface cysteines of FGF2 are not present in any other member of the FGF family secreted by the ER/Golgi-dependent pathway.

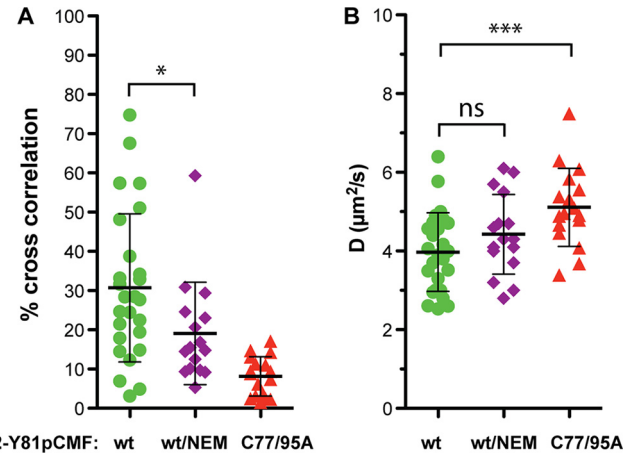

FIGURE 2. **Oligomerization of FGF2 variant forms on the surface of giant unilamellar vesicles analyzed by scanning cross-correlation fluorescence spectroscopy.** GUVs were prepared with a plasma-membrane-like lipid composition including 2 mol % $PI(4,5)P_2$. Three variant forms of FGF2, FGF2-Y81pCMF with wild-type cysteines, FGF2-Y81pCMF with alkylated cysteines (treatment with *N*-ethylmaleimide), and FGF2-Y81pCMF-C77A/C95A, were C-terminally labeled with Atto488 and Atto655 dyes employing sortagging (see "Experimental Procedures" for details). All three variants of FGF2 were incubated with GUVs as mixtures of two different FGF2 populations based upon the two different dyes. Cross-correlation curves were derived from a two-color analysis and used to compare the relative abundance of FGF2 oligomers under the conditions indicated (*panel A*). In addition, the data were used to calculate diffusion constants of FGF2 oligomers formed under the experimental conditions indicated (*panel B*). To test whether observed differences between experimental conditions were statistically significant, an unpaired two-tailed *t* test was performed (*ns* = not significant; * = p value ≤ 0.05; *** = p value ≤ 0.001). For further details see "Experimental Procedures."

DTT (Fig. 4*B*). By contrast, the amounts of monomers and dimers observed for FGF2-Y81pCMF with alkylated cysteines (Fig. 4*C*) or FGF2-Y81pCMF-C77A/C95A (Fig. 4*D*) remained unaffected after DTT treatment. This analysis also revealed the low abundance of higher oligomeric forms such as trimers and tetramers of FGF2-Y81pCMF with alkylated cysteines (Fig. 4*C*) or FGF2-Y81pCMF-C77A/C95A (Fig. 4*D*). Of note, however, under all experimental conditions, dimers of FGF2-Y81pCMF were observed that could not be converted into monomers using reducing reagents. Consistently, FGF2-Y81pCMF with alkylated cysteines and FGF2-Y81pCMF-C77A/C95A were also found to form dimers in the presence of $PI(4,5)P_2$-containing membranes, suggesting that these dimers can form in a disulfide-independent manner under native conditions. By contrast, formation of oligomers higher than dimers largely depended on disulfide bridge formation involving the two surface cysteines in position 77 and 95 of FGF2-Y81pCMF. The combined findings shown in Figs. 2–4 demonstrate that, in the presence of $PI(4,5)P_2$-containing membranes, FGF2 is recruited and undergoes controlled oligomerization in a time-dependent manner. It appears that formation of intermolecular disulfide bridges drives oligomerization, resulting in membrane-inserted forms that over time become partially resistant to reducing agents.

Functional Surface Cysteines of Phosphomimetic FGF2 Are Required for Efficient Membrane Pore Formation—Because oligomerization of FGF2 has been shown to be critical for $PI(4,5)P_2$-dependent membrane pore formation (10), we tested whether the two surface cysteines are required for membrane permeabilization mediated by FGF2 oligomers (Fig. 5). Similar to the scanning fluorescence cross-correlation (Fig. 2) and native gel experiments (Fig. 4) described above, three experimental conditions were used comparing FGF2-Y81pCMF with wild-type surface cysteines to FGF2-Y81pCMF with alkylated surface cysteines and FGF2-Y81pCMF-C77A/C95A. To test for membrane pore formation mediated by FGF2 oligomers, we used an established assay measuring membrane passage of a small fluorophore (10). As shown in Fig. 5*A*, substitution of the two surface cysteines by alanines (FGF2-Y81pCMF) caused a dramatically decreased ability of FGF2-Y81pCMF to form membrane pores in a $PI(4,5)P_2$-dependent manner. Similarly, treatment of FGF2-Y81pCMF with NEM to alkylate surface cysteines caused a concentration-dependent decrease of membrane permeabilization (Fig. 5*B*). At 4 μM NEM (molar ratio of FGF2 surface cysteines to NEM = 1), inhibition was almost complete, resulting in a very low activity similar to what was observed for FGF2-Y81pCMF-C77A/C95A. These findings demonstrate that functional surface cysteines are required for membrane pore formation by FGF2-Y81pCMF oligomers, suggesting that the formation of disulfide bridges drives oligomerization and membrane insertion of phosphomimetic FGF2.

FGF2 Variant Forms Lacking Surface Cysteines Are Not Secreted from Cells—The combined results from the reconstitution experiments described above establish a role for the two surface cysteines in position 77 and 95 in the formation of disulfides required for $PI(4,5)P_2$-dependent oligomerization and membrane permeabilization of phosphomimetic FGF2. To test the significance of these findings in a cellular context, we conducted cell-based secretion experiments comparing the wild-type form of FGF2 with a variant in which both cysteines were replaced by alanines (Fig. 6). As a technical control, a secretion-defective variant form of FGF2 that is impaired in binding to both $PI(4,5)P_2$ and heparan sulfates (FGF2-K127Q/R128Q/K133Q) was used (9). All FGF2 variants were expressed as GFP fusion proteins in a doxycycline-dependent manner in stably transduced CHO cells. To quantify FGF2 secretion, a well established assay based on cell surface biotinylation followed by streptavidin affinity purification was used (13). This assay takes advantage of the fact that, after secretion, FGF2 is retained on cell surfaces bound to heparan sulfate proteoglycans. Employing a SDS-PAGE/Western analysis, both intracellular (non-biotinylated) and cell surface FGF2 (biotinylated) was quantified. Further controls included the detection of cytosolic proteins with glyceraldehyde-3-phosphate dehydrogenase (GAPDH) as an endogenous factor as well as exogenously expressed GFP. These experiments revealed that, relative to the wild-type form of FGF2, secretion to cell surfaces of FGF2 is severely impaired when the two surface cysteines are replaced by alanines (Fig. 6*A*, *lane 2 versus lane 4*). This phenotype was in fact even stronger than the one observed with a FGF2 mutant impaired in $PI(4,5)P_2$ binding (Fig. 6*A*, *lane 6*). Although FGF2-C77A/C95A was hardly detectable on cell surfaces, ~25% of FGF2-K127Q/R128Q/K133Q was found secreted compared with the wild-type form of FGF2 (Fig. 6*B*). The significance of these findings was further corroborated by the fact that neither GAPDH nor GFP was detectable in the fraction of biotinylated proteins. These results suggest that the dependence on surface cysteines

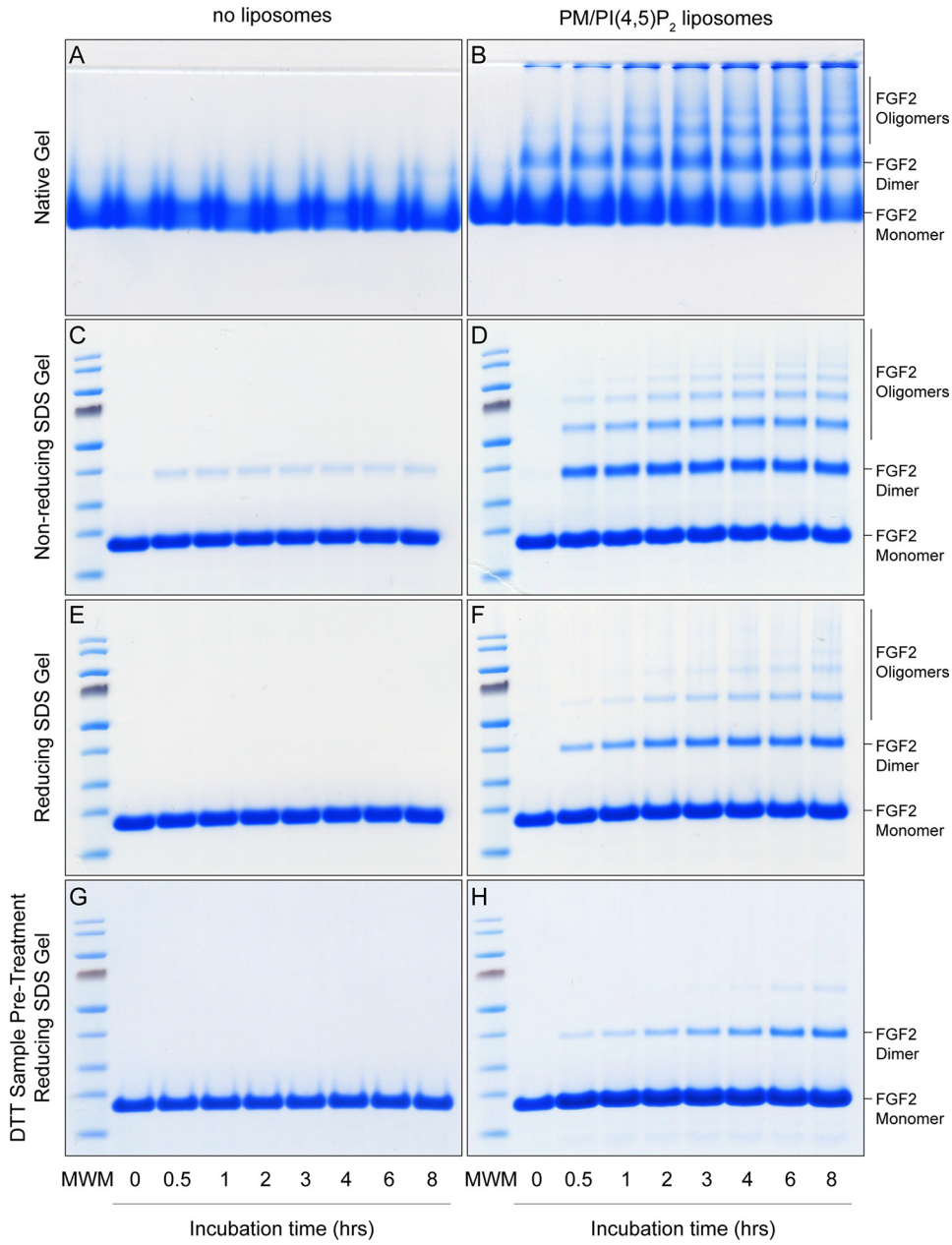

FIGURE 3. **Analysis of membrane-associated FGF2 oligomers by native gel electrophoresis as well as non-reducing and reducing SDS-PAGE.** FGF2-Y81pCMF was incubated either in the absence of liposomes (*panels A, C, E,* and *F*) or with liposomes containing a plasma-membrane (PM)-like lipid composition including 2 mol % $PI(4,5)P_2$ (*panels B, D, F,* and *H*) for the times indicated. After detergent extraction, membrane-bound material was analyzed either on a native gel system developed for the separation of basic proteins (*panels A* and *B*; see "Experimental Procedures" for details), on non-reducing SDS gels (*panels C* and *D*), or on reducing SDS gels (*panels E* and *F*). In addition, FGF2 samples pretreated with 10 mM DTT before incubation under the conditions indicated were analyzed on reducing SDS gels (*panels G* and *H*). The molecular weight markers (*MWM*) used on SDS gels correspond to 15, 25, 30, 40, 50, 70 (*dark blue*), 80, 115, and 140 kDa, respectively. In all experiments, before membrane extraction with detergent, samples were treated with NEM to block free thiols, preventing disulfide formation during sample processing. All gels were stained with Coomassie InstantBlue (Expedeon).

for $PI(4,5)P_2$-dependent oligomerization and membrane insertion of FGF2 observed in *in vitro* reconstitution experiments is directly relevant for FGF2 secretion from cells.

Rerouting of a Signal-peptide-containing FGF Family Member into the Unconventional Secretory Pathway of FGF2—To challenge the conclusions from both reconstitution and cell-based experiments shown in Figs. 2–6, we asked whether molecular determinants required for FGF2 secretion are transplantable. Based on a similar overall fold compared with FGF2 (Fig. 1, *A* and *B*), we selected FGF4 for these experiments, a signal-peptide-containing FGF family member that is secreted via the ER/Golgi-dependent pathway. For comparison with FGF2, five constructs based on FGF4 were generated as GFP fusion proteins (Fig. 7). This included a version containing the authentic amino acid sequence of FGF4 (*SP-FGF4-GFP*; Fig. 7, *A–D*) and a corresponding variant form without signal peptide (*FGF4-GFP*; Fig. 7, *E–H*). Furthermore, a construct representing a hybrid between FGF4 and FGF2 was generated containing all known molecular determinants required for FGF2 secretion in the context of the amino acid sequence of FGF4 (*FGF4/2-*

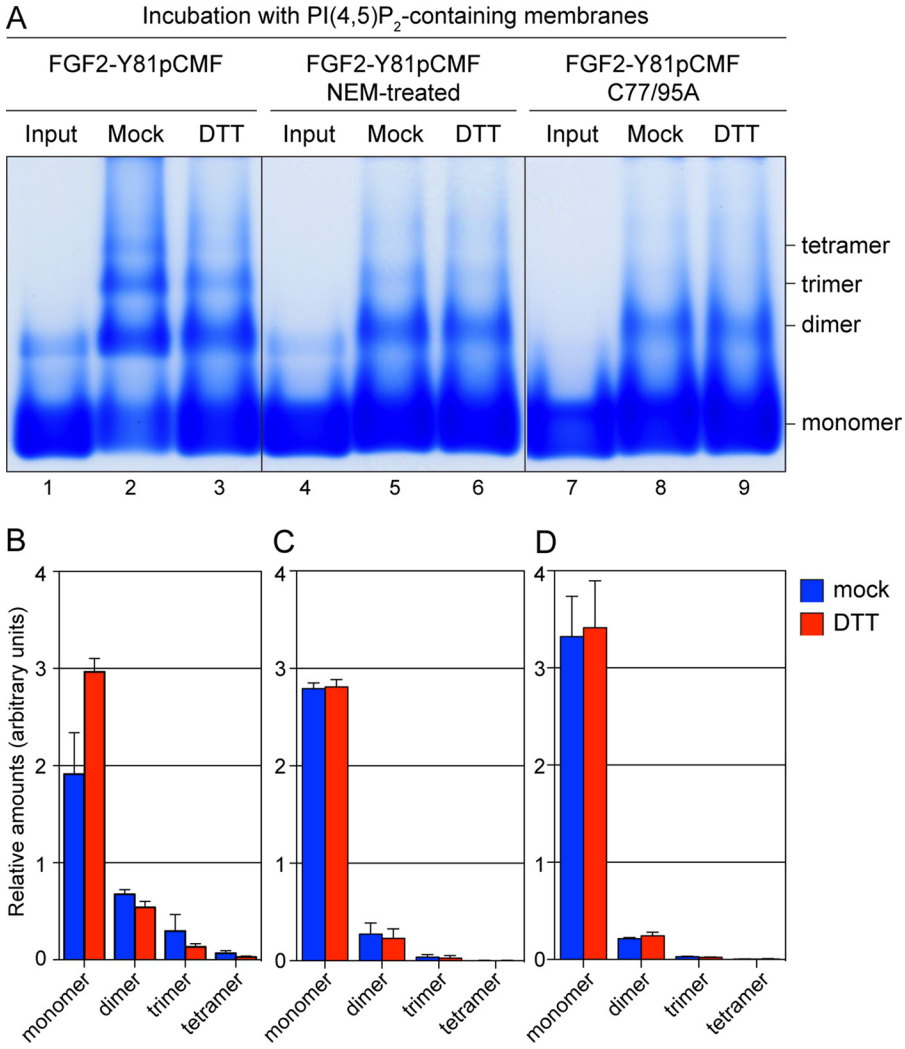

FIGURE 4. **Chemical alkylation and substitution of surface cysteines by alanines impairs formation of FGF2 oligomers higher than dimers.** Native gel electrophoresis was employed to analyze FGF2 oligomer formation under the conditions indicated. Three variant forms of FGF2, FGF2-Y81pCMF, FGF2-Y81pCMF with alkylated surface cysteines, and FGF2-Y81pCMF-C77A/C95A, were incubated with liposomes containing a plasma-membrane-like lipid composition including 2 mol % $PI(4,5)P_2$. After 6 h of incubation, samples were subjected to protein extraction with detergent. Where indicated, samples were treated with DTT to break disulfide bonds before native gel electrophoresis. All gels were stained with Coomassie InstantBlue (Expedeon). *Panel A* provides a representative example for the analysis on native gels of FGF2-Y81pCMF, FGF2-Y81pCMF with alkylated surface cysteines, and FGF2-Y81pCMF-C77A/C95A under the conditions indicated. *Panels B*, *C*, and *D* provide quantification of monomers, dimers, trimers, and tetramers under all experimental conditions using the LI-COR imaging platform. The statistical analysis is based on three independent experiments. Standard deviations are shown.

GFP; Fig. 7, *I–L*). This included tyrosine 81 (16), a basic stretch of amino acids required for $PI(4,5)P_2$ binding (including lysine 127 and arginine 128 as well as lysine 133) (9) and the two surface cysteines in position 77 and 95. To test a potential specific role of the two surface cysteines, two additional constructs were generated where the surface cysteines were either included into the background of FGF4-GFP (*FGF4-(+Cys)-GFP*; Fig. 7, *M–P*) or removed from the FGF4/2 hybrid protein (*FGF4/2-(−Cys)-GFP*; Fig. 7, *Q–T*). Stable CHO cell lines were generated by retroviral transduction expressing these constructs in a doxycycline-dependent manner. For comparison, a CHO cell line expressing FGF2-GFP in a doxycycline-dependent manner (25) was used (*FGF2-GFP*; Fig. 7, *U–X*). After induction of protein expression by doxycycline, all constructs were first analyzed for intracellular distribution. As expected, SP-FGF4-GFP was detected in a perinuclear region colocalizing with a Golgi marker (Fig. 7, *A–D*). By contrast, FGF4-GFP (Fig. 7, *E–H*), FGF4/2-GFP (Fig. 7, *I–L*), FGF4-(+Cys)-GFP (Fig. 7, *M–P*), FGF4/2-(-Cys)-GFP (Fig. 7, *Q–T*), and FGF2-GFP (Fig. 7, *U–X*) were mainly found in the cytoplasm and the nucleus. Interestingly, all constructs representing different kinds of hybrids between FGF2 and FGF4 were strongly detectable at the plasma membrane, a phenomenon that was only occasionally observed for FGF2-GFP and FGF4-GFP. We next analyzed the efficiency of secretion of each of these fusion proteins (Fig. 8). In addition to surface biotinylation experiments as shown in Fig. 6, the cellular supernatants were analyzed as well (Fig. 8*A*) and the extracellular amounts of each fusion protein were quantified relative to the extracellular population of FGF2-GFP (Fig. 8*B*). As expected, ER/Golgi-dependent secretion of SP-FGF4-GFP was highly efficient with the majority of the fusion protein secreted into the cellular supernatant (Fig. 8*B*). By contrast, consistent with earlier findings (12, 13), the extracellular population of FGF2-GFP was retained on cell surfaces.

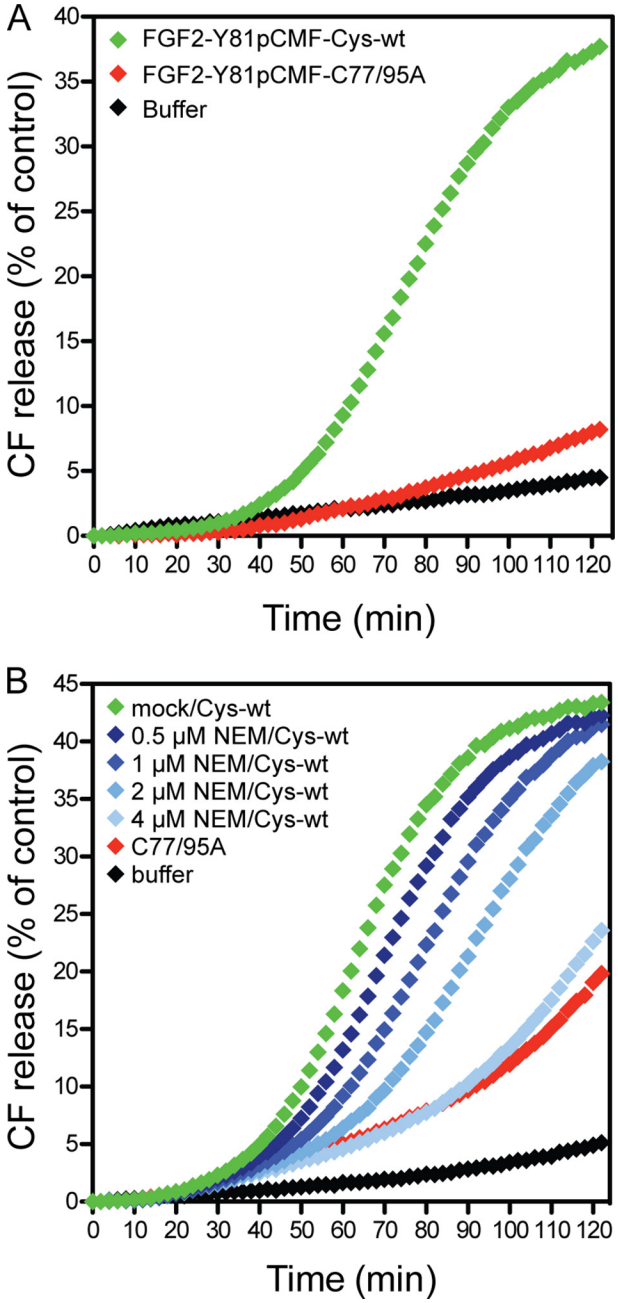

FIGURE 5. **Membrane pore formation mediated by FGF2-Y81pCMF depends on functional surface cysteines.** Carboxyfluorescein (*CF*) was sequestered in liposomes containing a plasma-membrane-like lipid composition containing 2 mol % $PI(4,5)P_2$. Liposomes were incubated with either FGF2-Y81pCMF (*panels A* and *B*), FGF2-Y81pCMF-C77A/C95A (*panels A* and *B*), or FGF2-Y81pCMF with alkylated surface cysteines (NEM treatment; *panel B*) as indicated. At the highest concentration of 4 μM NEM, the ratio of the two surface cysteines at 2 μM FGF2 to NEM equals 1. Membrane pore formation was analyzed by measuring the release of luminal carboxyfluorescein quantified by fluorescence dequenching as described under "Experimental Procedures." The results shown are representative of five independent experiments.

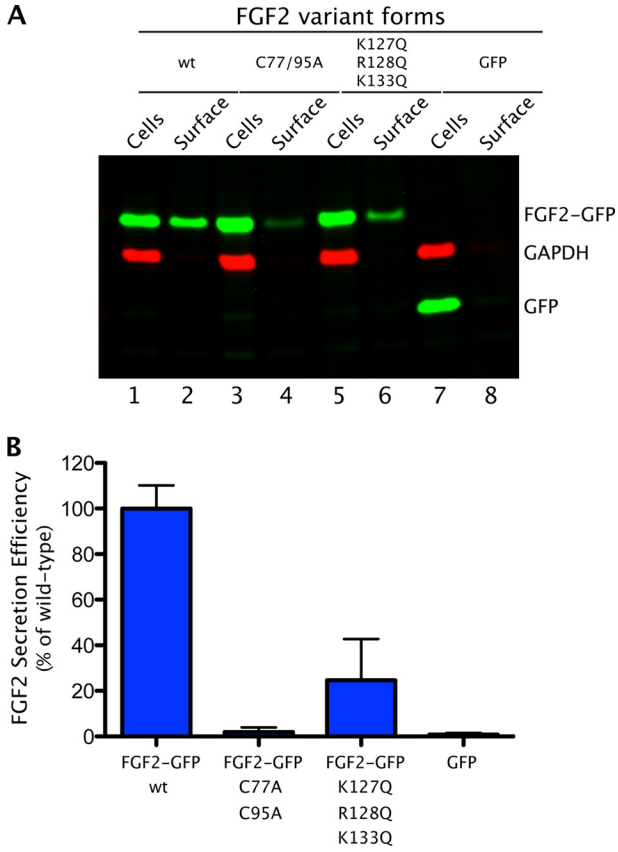

FIGURE 6. **FGF2 secretion from cells depends on functional surface cysteines.** CHO cells stably expressing either FGF2-GFP, FGF2-C77A/C95A-GFP, FGF2-K127Q/R128Q/K133Q-GFP, or GFP in a doxycycline-dependent manner were induced for protein expression for 16 h at 37 °C. Cells were incubated with a membrane-impermeable biotinylation reagent targeting primary amines of cell surface proteins. After quenching and detergent-mediated cell lysis, biotinylated material was purified using streptavidin beads. Aliquots from the non-biotinylated fractions (10%; corresponding to intracellular population) and the biotinylated fractions (50%); corresponding to the secreted population) were subjected to SDS-PAGE and Western blotting using anti-GFP primary antibodies. In addition, all fractions were analyzed for an endogenous marker, GAPDH (*panel A*). Antigens were detected and quantified using an Odyssey infrared imaging system (LI-COR Biosciences). Signals derived from biotinylated FGF2 variant forms corresponding to the secreted cell surface population were normalized based on FGF2 wild type that was set to 100% (*panel B*).

The variant of FGF4-GFP without signal peptide was only found in very small amounts on cell surfaces and was absent from cellular supernatants. Importantly, this lack of secretion in the absence of a signal peptide was reversed in FGF4/2-GFP that was found secreted with even better efficiency than FGF2-GFP (Fig. 8*B*). Most intriguingly, the whole population of secreted FGF4/2-GFP was found associated with cell surfaces, a hallmark of unconventional secretion of FGF2. To test a specific role for the surface cysteines the cell surface population of FGF4/2-(−Cys)-GFP and FGF4-(+Cys)-GFP was analyzed. As opposed to the strong secretion defect observed upon removal of surface cysteines from authentic FGF2 (Fig. 6), the efficiency of secretion of FGF4/2-GFP and FGF4/2-(−Cys)-GFP was found to be similar (Fig. 8*B*). This might be due to the high overall efficiency of secretion of the FGF4/2 hybrid protein (Fig. 8) and its strong association with the plasma membrane, a phenomenon that is less pronounced for authentic FGF2 (Fig. 7). However, inserting the two surface cysteines into FGF4-GFP (FGF4-(+Cys)-GFP) caused a strong increase in unconventional secretion (Fig. 8, *A* and *B*), demonstrating a specific role of the two surface cysteines of FGF2 in this process. In conclusion, transplanting key *cis* elements for unconventional secretion of FGF2 into a variant form of FGF4 without signal peptide

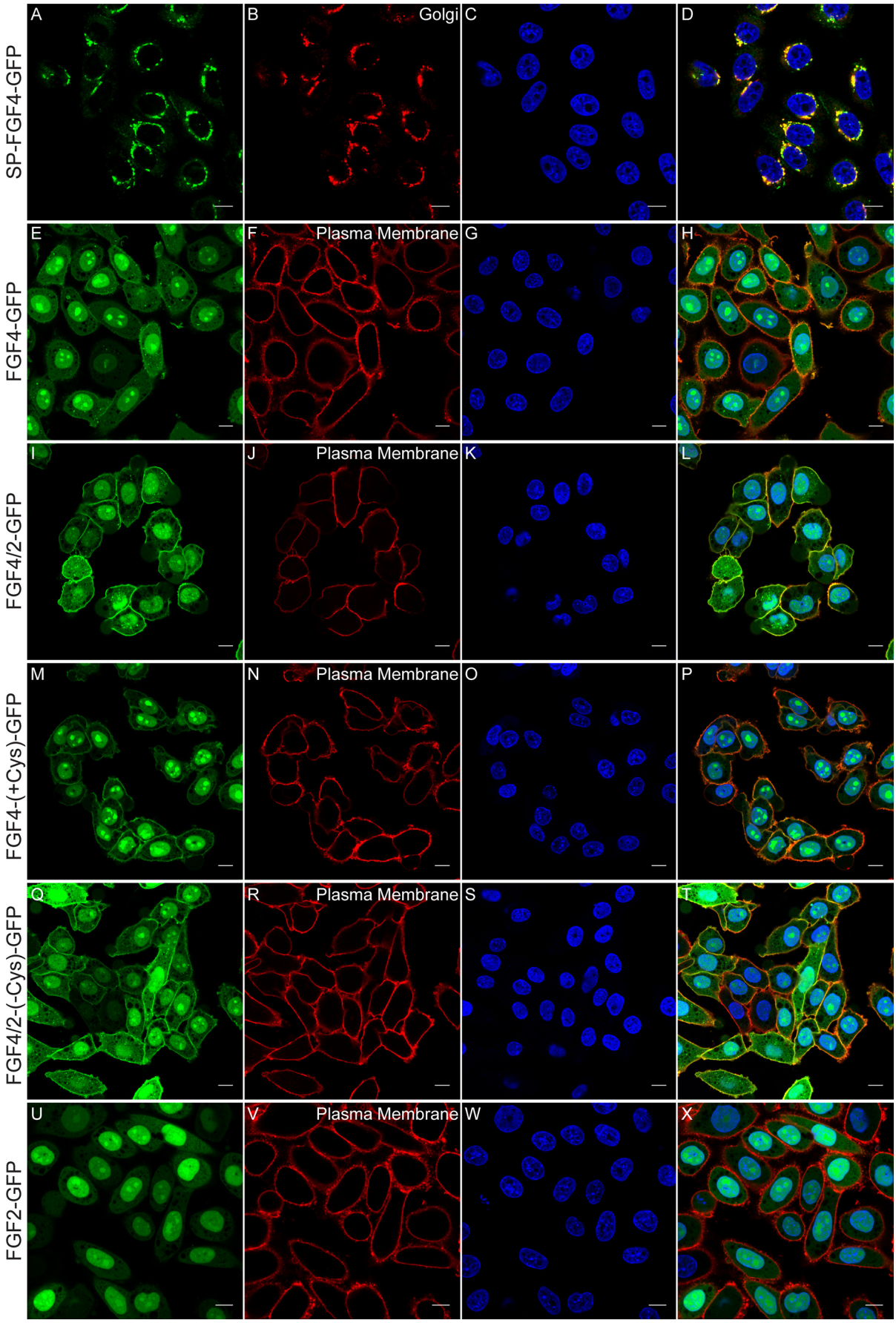
SP-FGF4-GFP
FGF4-GFP
FGF4/2-GFP
FGF4-(+Cys)-GFP
FGF4/2-(-Cys)-GFP
FGF2-GFP
A
B
Golgi
C
D
E
F
Plasma Membrane
G
H
I
J
Plasma Membrane
K
L
M
N
Plasma Membrane
O
P
Q
R
Plasma Membrane
S
T
U
V
Plasma Membrane
W
X

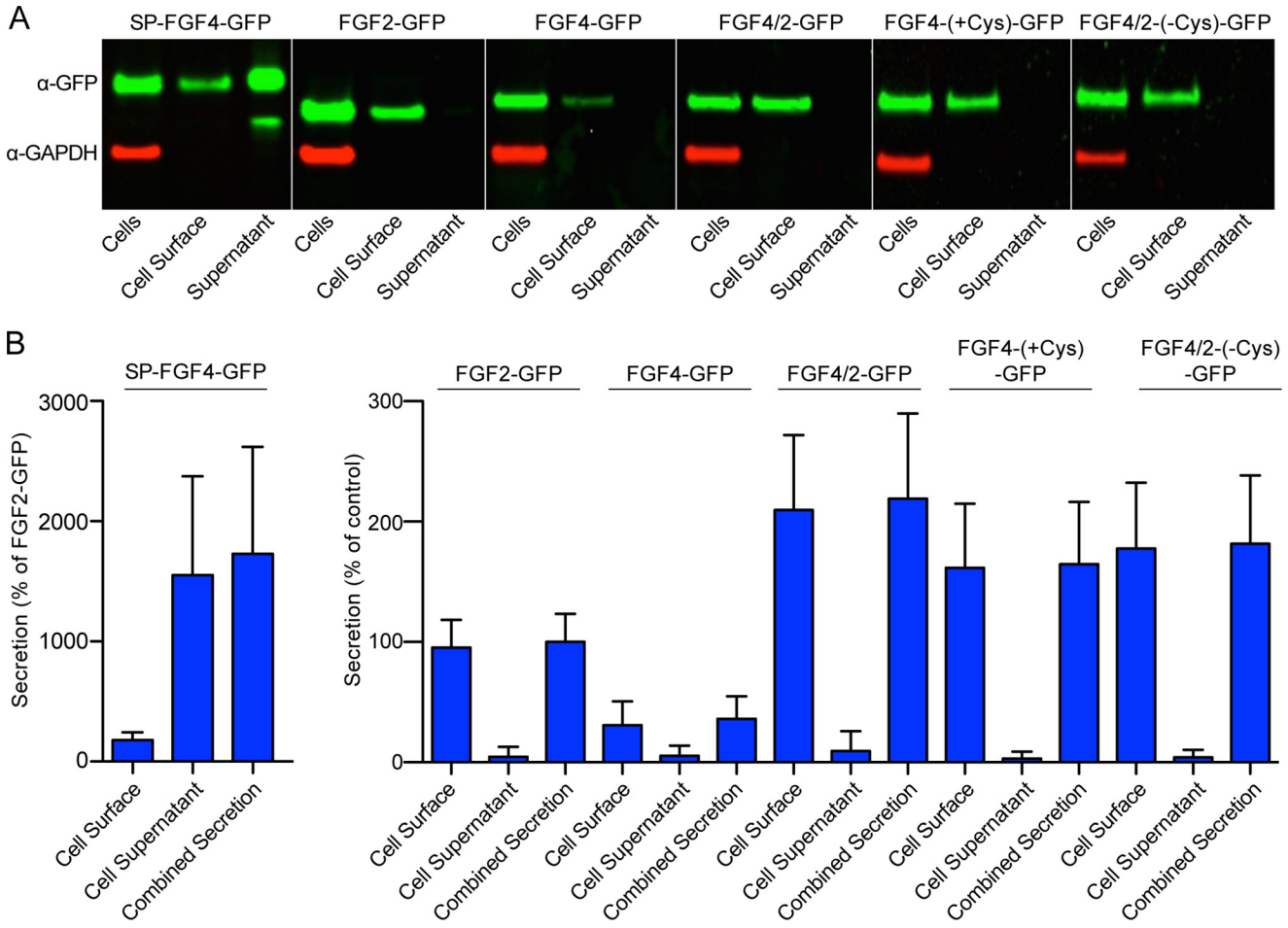

FIGURE 8. ***Cis* elements required for FGF2 membrane translocation are transplantable and redirect a signal peptide-lacking variant form of FGF4 to the unconventional secretory pathway of FGF2.** The efficiency of secretion of the various fusion proteins indicated was compared by a combination of cell surface biotinylation (as introduced in Fig. 6) and heparin affinity purification from cellular supernatants. Stable CHO cell lines were cultivated for 24 h in the presence of 1 μg/ml doxycycline to induce the expression of the fusion proteins indicated. Heparin affinity chromatography was used to collect FGF fusion proteins present in cellular supernatants. Cells were surface-biotinylated as described under "Experimental Procedures" followed by affinity purification using streptavidin beads. For each cell line, the amounts of the FGF fusion proteins indicated present in cells (10% loaded), on cell surfaces (33% loaded), and in cellular supernatants (33% loaded) were analyzed by SDS-PAGE and quantitative Western blotting using the LI-COR imaging platform. *Panel A* shows the results from a representative experiment with GAPDH as an intracellular control protein not present on cell surfaces or in cellular supernatants. *Panel B* provides a statistical analysis with standard deviations calculated from three independent experiments with the amount of FGF2-GFP on cell surfaces set as a reference point (=100%).

results in unconventional secretion along with retention on cell surfaces.

DISCUSSION

The molecular mechanism by which FGF2 translocates across plasma membranes to reach the extracellular space by an ER/Golgi-independent pathway is beginning to emerge. Previous studies established that recruitment to the inner leaflet mediated by the phosphoinositide $PI(4,5)P_2$ triggers oligomerization of FGF2 concomitant with the formation of a lipidic membrane pore (7, 10). Membrane-inserted FGF2 oligomers have been interpreted as translocation intermediates that are resolved by cell surface heparan sulfate proteoglycans (11). Cell surface heparan sulfate proteoglycans act as a trap to ensure directional transport of FGF2 into the extracellular space (12, 13). However, the structure-function relationship of membrane-inserted FGF2 oligomers and molecular determinants of their formation are unknown. The current study now provides the first insights into how FGF2 subunits assemble to insert into the plasma membrane. Despite a high degree of structural similarities between members of the FGF family, two surface cysteines in position 77 and 95 are highly conserved in all mammalian forms of FGF2 but are absent from all FGF family members containing N-terminal signal peptides for ER/Golgi-dependent secretion. By contrast, two other cysteines in FGF2 in positions 33 and 100 are highly conserved among all FGF

FIGURE 7. **Localization of various FGF-GFP fusion proteins as analyzed by confocal microscopy.** Constructs encoding various kinds of FGF-GFP fusion proteins were used to generate stable CHO cell lines by retroviral transduction (25). Upon protein expression in the presence of doxycycline subcellular localization of the FGF fusion proteins indicated was analyzed by confocal microscopy (*panels A*, *E*, *I*, *M*, *Q*, and *U*). For colocalization experiments, either the Golgi marker GM-130 (*panel B*) or wheat germ agglutinin (*panels F*, *J*, *N*, *R*, and *V*) as a plasma membrane marker was used. In addition, nuclei were stained with DAPI (*panels C*, *G*, *K*, *O*, *S*, and *W*), and merged images were generated (*panels D*, *H*, *L*, *P*, *T*, and *X*). The following constructs were analyzed: SP-FGF4-GFP (authentic FGF4 with a signal peptide; *panels A–D*), FGF4-GFP without signal peptide (*panels E–H*), a FGF4/2-GFP hybrid protein (*panels I–L*), FGF4-(+Cys)-GFP (*panels M-P*), FGF4/2-(−Cys)-GFP (*panels Q–T*), and FGF2-GFP (*panels U-X*). *Scale bars* = 100 nm.

family members, suggesting that they are of general importance for the overall structure of FGF proteins. Therefore, the unique presence of two surface cysteines in FGF2 suggested a specific role in unconventional secretion. In the current study we demonstrated that cysteine 77 and cysteine 95 are engaged in the formation of disulfide bridges whose formation drives $PI(4,5)P_2$-dependent oligomerization of FGF2. This is shown by alkylation of surface cysteines using NEM or by their substitution with alanines. Intriguingly, under these experimental conditions, membrane pore formation of FGF2 was largely impaired as well. The relevance of these reconstitution experiments was shown in cells with a FGF2 variant form lacking the two surface cysteines in positions 77 and 95 not being secreted. Therefore, combined with earlier studies, three *cis* elements important for FGF2 secretion have been identified with (i) a stretch of basic residues that form the binding pocket for $PI(4,5)P_2$ (9), (ii) a tyrosine residue phosphorylated by Tec kinase(16), and (iii) two surface cysteines involved in FGF2 oligomerization and membrane pore formation (this study). To challenge these findings, we sought to test whether these *cis* elements are transplantable to redirect a secretory protein from the ER/Golgi-dependent secretory pathway into the unconventional secretory pathway of FGF2. The experiments shown in Figs. 7 and 8 demonstrate that after removal of its signal peptide, FGF4 was secreted unconventionally when the three elements described above were transplanted into the equivalent positions known from FGF2. Strikingly, this process resulted in the presence of the FGF4/2 hybrid protein on cell surfaces, a hallmark of FGF2 secretion. By contrast, signal-peptide-dependent FGF4 secretion via the ER/Golgi-mediated pathway mainly resulted in secretion into cellular supernatants.

Based on previous findings and the results from the current study, we propose that FGF2 remains reduced as a monomer as long as it is present in the reducing redox environment of the cytoplasm (28, 29). However, upon $PI(4,5)P_2$-dependent recruitment at the inner leaflet of the plasma membrane, we propose that FGF2 encounters a different microenvironment that allows for the formation of intermolecular disulfide bridges. In particular, during insertion into the membrane, FGF2 may get shielded from the reducing power of the cytoplasm. Therefore, the combination of $PI(4,5)P_2$-dependent recruitment and disulfide-dependent membrane pore formation is likely to represent the molecular basis for the specific targeting of FGF2 to the plasma membrane, a process that leads to oligomerization and membrane insertion concomitant with the translocation of FGF2 to cell surfaces.

Acknowledgment—We thank the Nikon Imaging Center for providing access to its core facility at Heidelberg University.

REFERENCES

1. Presta, M., Dell'Era, P., Mitola, S., Moroni, E., Ronca, R., and Rusnati, M. (2005) Fibroblast growth factor/fibroblast growth factor receptor system in angiogenesis. *Cytokine Growth Factor Rev.* **16,** 159–178
2. Pardo, O. E., Wellbrock, C., Khanzada, U. K., Aubert, M., Arozarena, I., Davidson, S., Bowen, F., Parker, P. J., Filonenko, V. V., Gout, I. T., Sebire, N., Marais, R., Downward, J., and Seckl, M. J. (2006) FGF-2 protects small cell lung cancer cells from apoptosis through a complex involving PKCϵ, B-Raf, and S6K2. *EMBO J.* **25,** 3078–3088
3. Nickel, W. (2011) The unconventional secretory machinery of fibroblast growth factor 2. *Traffic* **12,** 799–805
4. Nickel, W., and Rabouille, C. (2009) Mechanisms of regulated unconventional protein secretion. *Nat. Rev. Mol. Cell Biol.* **10,** 148–155
5. Wegehingel, S., Zehe, C., and Nickel, W. (2008) Rerouting of fibroblast growth factor 2 to the classical secretory pathway results in post-translational modifications that block binding to heparan sulfate proteoglycans. *FEBS Lett.* **582,** 2387–2392
6. Nickel, W. (2003) The mystery of nonclassical protein secretion. A current view on cargo proteins and potential export routes. *Eur. J. Biochem.* **270,** 2109–2119
7. Rabouille, C., Malhotra, V., and Nickel, W. (2012) Diversity in unconventional protein secretion. *J. Cell Sci.* **125,** 5251–5255
8. Zhang, M., and Schekman, R. (2013) Cell biology. Unconventional secretion, unconventional solutions. *Science* **340,** 559–561
9. Temmerman, K., Ebert, A. D., Müller, H. M., Sinning, I., Tews, I., and Nickel, W. (2008) A direct role for phosphatidylinositol 4,5-bisphosphate in unconventional secretion of fibroblast growth factor 2. *Traffic* **9,** 1204–1217
10. Steringer, J. P., Bleicken, S., Andreas, H., Zacherl, S., Laussmann, M., Temmerman, K., Contreras, F. X., Bharat, T. A., Lechner, J., Müller, H. M., Briggs, J. A., García-Sáez, A. J., and Nickel, W. (2012) Phosphatidylinositol 4,5-bisphosphate (PI(4,5)P2)-dependent oligomerization of fibroblast growth factor 2 (FGF2) triggers the formation of a lipidic membrane pore implicated in unconventional Secretion. *J. Biol. Chem.* **287,** 27659–27669
11. Steringer, J. P., Muller, H. M., and Nickel, W. (2014) Unconventional secretion of fibroblast growth factor 2: a novel type of protein translocation across membranes? *J. Mol. Biol.* 10.1016/j.jmb.2014.07.012
12. Nickel, W. (2007) Unconventional secretion: an extracellular trap for export of fibroblast growth factor 2. *J. Cell Sci.* **120,** 2295–2299
13. Zehe, C., Engling, A., Wegehingel, S., Schäfer, T., and Nickel, W. (2006) Cell-surface heparan sulfate proteoglycans are essential components of the unconventional export machinery of FGF-2. *Proc. Natl. Acad. Sci. U.S.A.* **103,** 15479–15484
14. Backhaus, R., Zehe, C., Wegehingel, S., Kehlenbach, A., Schwappach, B., and Nickel, W. (2004) Unconventional protein secretion: membrane translocation of FGF-2 does not require protein unfolding. *J. Cell Sci.* **117,** 1727–1736
15. Torrado, L. C., Temmerman, K., Müller, H. M., Mayer, M. P., Seelenmeyer, C., Backhaus, R., and Nickel, W. (2009) An intrinsic quality-control mechanism ensures unconventional secretion of fibroblast growth factor 2 in a folded conformation. *J. Cell Sci.* **122,** 3322–3329
16. Ebert, A. D., Laussmann, M., Wegehingel, S., Kaderali, L., Erfle, H., Reichert, J., Lechner, J., Beer, H. D., Pepperkok, R., and Nickel, W. (2010) Tec kinase-mediated phosphorylation of fibroblast growth factor 2 is essential for unconventional secretion. *Traffic* **11,** 813–826
17. Bradshaw, J. M. (2010) The Src, Syk, and Tec family kinases: distinct types of molecular switches. *Cell. Signal.* **22,** 1175–1184
18. Liu, P., Cheng, H., Roberts, T. M., and Zhao, J. J. (2009) Targeting the phosphoinositide 3-kinase pathway in cancer. *Nat. Rev. Drug Discov.* **8,** 627–644
19. Nickel, W., and Seedorf, M. (2008) Unconventional mechanisms of protein transport to the cell surface of eukaryotic cells. *Annu. Rev. Cell Dev. Biol.* **24,** 287–308
20. Young, T. S., Ahmad, I., Yin, J. A., and Schultz, P. G. (2010) An enhanced system for unnatural amino acid mutagenesis in *E. coli*. *J. Mol. Biol.* **395,** 361–374
21. Antos, J. M., Chew, G. L., Guimaraes, C. P., Yoder, N. C., Grotenbreg, G. M., Popp, M. W., and Ploegh, H. L. (2009) Site-specific N- and C-terminal labeling of a single polypeptide using sortases of different specificity. *J. Am. Chem. Soc.* **131,** 10800–10801
22. García-Sáez, A. J., Ries, J., Orzáez, M., Pérez-Payà, E., and Schwille, P. (2009) Membrane promotes tBID interaction with BCL(XL). *Nat. Struct. Mol. Biol.* **16,** 1178–1185
23. Temmerman, K., and Nickel, W. (2009) A novel flow cytometric assay to quantify interactions between proteins and membrane lipids. *J. Lipid Res.* **50,** 1245–1254

24. Reisfeld, R. A., Lewis, U. J., and Williams, D. E. (1962) Disk electrophoresis of basic proteins and peptides on polyacrylamide gels. *Nature* **195,** 281–283
25. Engling, A., Backhaus, R., Stegmayer, C., Zehe, C., Seelenmeyer, C., Kehlenbach, A., Schwappach, B., Wegehingel, S., and Nickel, W. (2002) Biosynthetic FGF-2 is targeted to non-lipid raft microdomains following translocation to the extracellular surface of CHO cells. *J. Cell Sci.* **115,** 3619–3631
26. García-Sáez, A. J., and Schwille, P. (2008) Fluorescence correlation spectroscopy for the study of membrane dynamics and protein/lipid interactions. *Methods* **46,** 116–122
27. Popp, M. W., Antos, J. M., Grotenbreg, G. M., Spooner, E., and Ploegh, H. L. (2007) Sortagging: a versatile method for protein labeling. *Nat. Chem. Biol.* **3,** 707–708
28. Hanschmann, E. M., Godoy, J. R., Berndt, C., Hudemann, C., and Lillig, C. H. (2013) Thioredoxins, glutaredoxins, and peroxiredoxins-molecular mechanisms and health significance: from cofactors to antioxidants to redox signaling. *Antioxid. Redox. Signal* **19,** 1539–1605
29. Lillig, C. H., and Berndt, C. (2013) Glutaredoxins in thiol/disulfide exchange. *Antioxid. Redox. Signal* **18,** 1654–1665